THE JOURNAL OF BIOLOGICAL CHEMISTRY VOL. 281, NO. 34, pp. 24566–24574, August 25, 2006
© 2006 by The American Society for Biochemistry and Molecular Biology, Inc. Printed in the U.S.A.

Matrix Metalloproteinase-9 Degrades Amyloid-β Fibrils *in Vitro* and Compact Plaques *in Situ*[*][S]

Received for publication, March 15, 2006, and in revised form, June 1, 2006 Published, JBC Papers in Press, June 20, 2006, DOI 10.1074/jbc.M602440200

Ping Yan[‡1], **Xiaoyan Hu**[‡1], **Haowei Song**[§], **Kejie Yin**[‡], **Randall J. Bateman**[‡], **John R. Cirrito**[‡], **Qingli Xiao**[‡], **Fong F. Hsu**[§], **John W. Turk**[§], **Jan Xu**[‡], **Chung Y. Hsu**[¶], **David M. Holtzman**[‡‖], **and Jin-Moo Lee**[‡2]

From the [‡]*Department of Neurology and the Hope Center for Neurological Disorders,* [§]*Division of Endocrinology, Diabetes, Metabolism, and Lipid Research, Department of Internal Medicine,* [‖]*Department of Molecular Biology and Pharmacology, Washington University School of Medicine, St. Louis, Missouri 63110 and the* [¶]*Taipei Medical University, Taipei, Taiwan*

The pathological hallmark of Alzheimer disease is the senile plaque principally composed of tightly aggregated amyloid-β fibrils (fAβ), which are thought to be resistant to degradation and clearance. In this study, we explored whether proteases capable of degrading soluble Aβ (sAβ) could degrade fAβ as well. We demonstrate that matrix metalloproteinase-9 (MMP-9) can degrade fAβ and that this ability is not shared by other sAβ-degrading enzymes examined, including endothelin-converting enzyme, insulin-degrading enzyme, and neprilysin. fAβ was decreased in samples incubated with MMP-9 compared with other proteases, assessed using thioflavin-T. Furthermore, fAβ breakdown with MMP-9 but not with other proteases was demonstrated by transmission electron microscopy. Proteolytic digests of purified fAβ were analyzed with matrix-assisted laser desorption ionization time-of-flight mass spectrometry to identify sites of Aβ that are cleaved during its degradation. Only MMP-9 digests contained fragments ($A\beta_{1-20}$ and $A\beta_{1-30}$) from $fA\beta_{1-42}$ substrate; the corresponding cleavage sites are thought to be important for β-pleated sheet formation. To determine whether MMP-9 can degrade plaques formed *in vivo*, fresh brain slices from aged APP/PS1 mice were incubated with proteases. MMP-9 digestion resulted in a decrease in thioflavin-S (ThS) staining. Consistent with a role for endogenous MMP-9 in this process *in vivo*, MMP-9 immunoreactivity was detected in astrocytes surrounding amyloid plaques in the brains of aged APP/PS1 and APPsw mice, and increased MMP activity was selectively observed in compact ThS-positive plaques. These findings suggest that MMP-9 can degrade fAβ and may contribute to ongoing clearance of plaques from amyloid-laden brains.

One of the key pathological features of Alzheimer disease (AD)[3] is the senile plaque, extracellular deposits found throughout the brains of AD patients, composed primarily of the amyloid-β peptide (Aβ). Aggregated Aβ in senile plaques can be found in two conformations: non-β-pleated-sheet (non-fibrillar) conformation, known as "diffuse plaques" or β-pleated sheet (fibrillar) conformation, known as "compact plaques" (1).

The 42-amino acid peptide ($A\beta_{1-42}$), the predominant peptide length found in senile plaques, has a remarkable propensity to aggregate at high concentrations to form a β-pleated sheet structure (2, 3). This is generally viewed as an irreversible process resulting in the formation of fibrillar Aβ (fAβ), which is insoluble and resistant to proteolysis, endowing compact plaques with a resistance to degradation and clearance. Given the purported irreversibility of Aβ fibril formation and the resistance to degradation, one might expect that senile plaques would continue to grow throughout disease progression; however, careful observational studies indicate that plaque size remains relatively constant over a wide range of disease durations (4). In addition, *in vivo* imaging in the APPsw (Tg2576) transgenic mouse model of Alzheimer's disease (using multiphoton microscopy) demonstrated that plaques remain constant in size over a period of many months (5). These observations have led some to believe that plaques, once formed, are in dynamic equilibrium with their environment, balancing formation with degradation (6). In support of this idea, a few isolated plaques in APPsw mice were found to decrease in size (5), raising the possibility that endogenous mechanisms for plaque clearance may exist. Moreover, a semiquantitative analysis of plaque burden in Alzheimer disease cases revealed that the most advanced cases (by Braak staging) actually had a slightly lower frequency of plaques than less advanced cases (7).

While plaques and amyloid fibrils have been viewed by some as resistant to proteolytic degradation, it is possible that certain (as yet unidentified) proteases may contribute to endogenous mechanisms leading to plaque clearance. A growing list of proteases are known to degrade soluble Aβ (sAβ) *in vitro*, including NEP (8), IDE (9), ECE (10), angiotensin-converting enzyme

* This work was supported by United States Public Health Service Grants P41-RR00954, P60-DK20579, and P30-DK56341 (to J. W. T.) and by National Institutes of Health Grants AG13956 (to D. M. H.) and NS048283 (to J.-M. L.). The costs of publication of this article were defrayed in part by the payment of page charges. This article must therefore be hereby marked "*advertisement*" in accordance with 18 U.S.C. Section 1734 solely to indicate this fact.

[S] The on-line version of this article (available at http://www.jbc.org) contains supplemental Figs. 1–3.

[1] Both authors contributed equally to this work.

[2] To whom correspondence should be addressed: Dept. of Neurology and the Hope Center for Neurological Disorders, Washington University, 660 South Euclid Ave., Campus Box 8111, St. Louis, MO 63110. Tel.: 314-747-1138; Fax: 314-747-1345; E-mail: leejm@neuro.wustl.edu.

[3] The abbreviations used are: AD, Alzheimer disease; ECE, endothelin-converting enzyme; Aβ, amyloid-β peptide; fAβ, amyloid-β fibrils; sAβ, soluble Aβ; IDE, insulin-degrading enzyme; MMP-9, matrix metalloproteinase-9; MS, mass spectrometry; MALDI-TOF, matrix-assisted laser desorption ionization time-of-flight; NEP, neprilysin; TEM, transmission electron microscopy; ThS, thioflavin-S; ThT, thioflavin-T; TIMP, tissue inhibitors of MMP; Tricine, *N*-[2-hydroxy-1,1-bis(hydroxymethyl)ethyl]glycine; MES, 4-morpholineethanesulfonic acid; PBS, phosphate-buffered saline.

This is an Open Access article under the CC BY license.

(11), the plasmin system (12), and MMP-9 (13). Each of these proteases appears to have distinguishing Aβ cleavage sites, generating characteristic fragments. However, experimental evidence that these proteases degrade sAβ *in vivo* is available only for a few: gene deletion of NEP (14), ECE (15), or IDE (16) in mice resulted in increased steady-state levels of Aβ in brain, suggesting a role in regulating endogenous basal levels of Aβ *in vivo*. Although all of these proteases demonstrate the ability to degrade sAβ, none has been convincingly shown to degrade Aβ fibrils or compact plaques.

MMP-9, a zinc-dependent metalloprotease, has not been well studied with regards to its potential role in amyloid clearance. Initially synthesized as an inactive proenzyme, pro-MMP-9 is cleaved into an active form upon cellular release by other proteases (17); this property puts MMP-9 in a unique position to regulate extracellular Aβ levels. Once activated, MMP-9 can be regulated by interacting with endogenous tissue inhibitors of MMPs (TIMPs) (17). Although expressed at low basal levels in normal brain tissue, MMP-9 expression is induced in neurons, astrocytes, microglia, and vascular cells under a variety of pathological conditions (18–23). Its expression is increased in the brains of AD patients (13, 24). Moreover MMP-9 expression in astrocytes is induced in the presence of the Aβ peptide (25).

In this study, we investigated the possibility that certain sAβ-degrading proteases were capable of degrading fAβ and amyloid plaques. Specifically, we examined the well studied sAβ-degrading proteases, ECE, IDE, and NEP, as well as MMP-9. We further examined the expression and activity of fAβ-degrading proteases in the brains of transgenic mouse models of AD.

EXPERIMENTAL PROCEDURES

APP Transgenic Mice—Tg2576 (APPsw) and APP/PS1 mice, models of AD, were used in this study. The production, genotyping, and background strains of these mice have been described previously (26). Transgenic mice were compared with age-matched littermate wild-type controls. All experimental protocols were approved by the Animal Studies Committee at Washington University.

Aβ Preparation and Analysis—Synthetic human $A\beta_{1-42}$ (Bachem) or $A\beta_{1-40}$ (American Peptide), dissolved in dimethyl sulfoxide (Me_2SO, Sigma) to a concentration of 5 mM, was diluted in MQ water to a final concentration of 25 μM immediately prior to use. Analysis with Tris-Tricine gels indicate that the vast majority of Aβ in this preparation (referred to as sAβ) was in the monomer form (data not shown). To prepare Aβ fibrils (fAβ), 5 mM $A\beta_{1-42}$ or $A\beta_{1-40}$ in Me_2SO was diluted in 10 mM HCl to 100 μM (for $A\beta_{1-42}$) or 200 μM (for $A\beta_{1-40}$), vortexed for 30 s, and incubated at 37 °C for 5 days (27). For mass spectrometry (MS) experiments, fAβ was further purified by centrifugation at 14,000 × *g* for 30 min. Fibrils were confirmed by thioflavin-T (ThT) fluorescence and electron microscopy (see below). Some experiments were repeated using $A\beta_{1-42}$ from a different manufacturer (American Peptide). ThT assay: 10 μl of sample was added to 0.2 ml of 10 μM ThT in 50 mM glycine buffer (pH 10.5). Fluorescence intensity was monitored at λ_{ex} of 440 nm and λ_{em} of 530 nm (28).

Proteolytic Digestions—Human recombinant ECE, ICE, NEP, and MMP-9 (R&D Systems) were used for digestion reactions using the following buffers: ECE, 0.1 M MES, 0.1 M NaCl (pH 6.0); IDE, 50 mM Tris, 1 M NaCl (pH 7.5); NEP, 0.1 M MES (pH 6.5); MMP-9, 50 mM Tris-HCl (pH 7.5), 10 mM $CaCl_2$, 150 mM NaCl, 0.05% Brij 35. Pro-MMP-9 was activated with 1 mM *p*-aminophenylmercuric acetate at 37 °C for 24 h prior to use. For sAβ digestions, 100 nM protease was incubated with 2.5 μM sAβ at 37 °C for varying periods of time (4 h to 5 days), then analyzed by MS. For fAβ digestions (employing ThT or TEM), 200 nM protease was added to 10 μl of fAβ in reaction buffer and incubated at 37 °C for 4 h to 5 days. After digestion, the reaction was analyzed by ThT assay or TEM. For fAβ digestions (employing MS), 10 μl of fAβ was applied to a Microcon 50-kDa centrifugal ultrafiltration unit (YM-50, Millipore) and washed with 500 μl of 10 mM HCl three times, then equilibrated with 500 μl of MQ water. Thirty μl of reaction buffer was added to the fAβ (retentate) and centrifuged; the filtrate was analyzed by MS (see below) to ensure that any contaminating Aβ monomer or fragments were washed away. Ten μl of 300 nM protease and 20 μl of reaction buffer was added to the fAβ (retentate) and incubated at 37 °C for 24 h, then centrifuged and analyzed by MS to detect liberated fragments of fAβ.

Mass Spectrometry—Samples were first passed through a reverse phase C18 Ziptip (Millipore), according to the manufacturer's instructions, then diluted 1:1 with matrix solution (a saturated solution of 3,5-dimethoxy-4-hydroxycinnamic acid in 50% acetonitrile with 0.1% trifluoroacetic acid in water), loaded onto a plate, and allowed to dry. The sample was then analyzed on an Applied Biosystesms (Foster City, CA) Voyager DE-STR matrix-assisted laser desorption-ionization time-of-flight mass spectrometer (MALDI-TOF MS) operated in linear mode. Insulin was used as an internal standard, and a calibration line constructed from its $[M + H]^+$ and $[M + 2H]^{2+}$ ions was used for quantification (29).

Electron Microscopy—Small volumes (5 μl) of fAβ samples were absorbed onto glow-discharged, carbon-coated, formvar/carbon-filmed 150-mesh copper grids. Grids were stained with 0.5% uranyl acetate and dried in a light-protected environment overnight before being viewed in a TEM (H-7500) operated at 80 kV (30).

In Situ Plaque Degradation—Brains were removed from anesthetized 9-month-old APP/PS1 mice after perfusion with cold saline and snap-frozen on dry ice. Five-μm cryostat sections were collected on slides. Every other section was flipped 180° so that identical faces of adjacent sections were exposed. Paired adjacent sections (one incubated with buffer, the other with 70 nM protease) were incubated at 37 °C for 5 days, stained with thioflavin-S (ThS) (31), then imaged with fluorescence microscopy (Olympus BX60). Using a 20× objective lens, identical fields from paired sections were photographed (precise alignment was confirmed by superimposing plaque staining patterns). The area of ThS fluorescence was determined using image analysis software (Sigma Scan) and expressed as a fraction of total area. Fractional area was compared between paired sections. The specific activities (Aβ degrading activity) of all proteases were approximately equivalent (Fig. 2*C*).

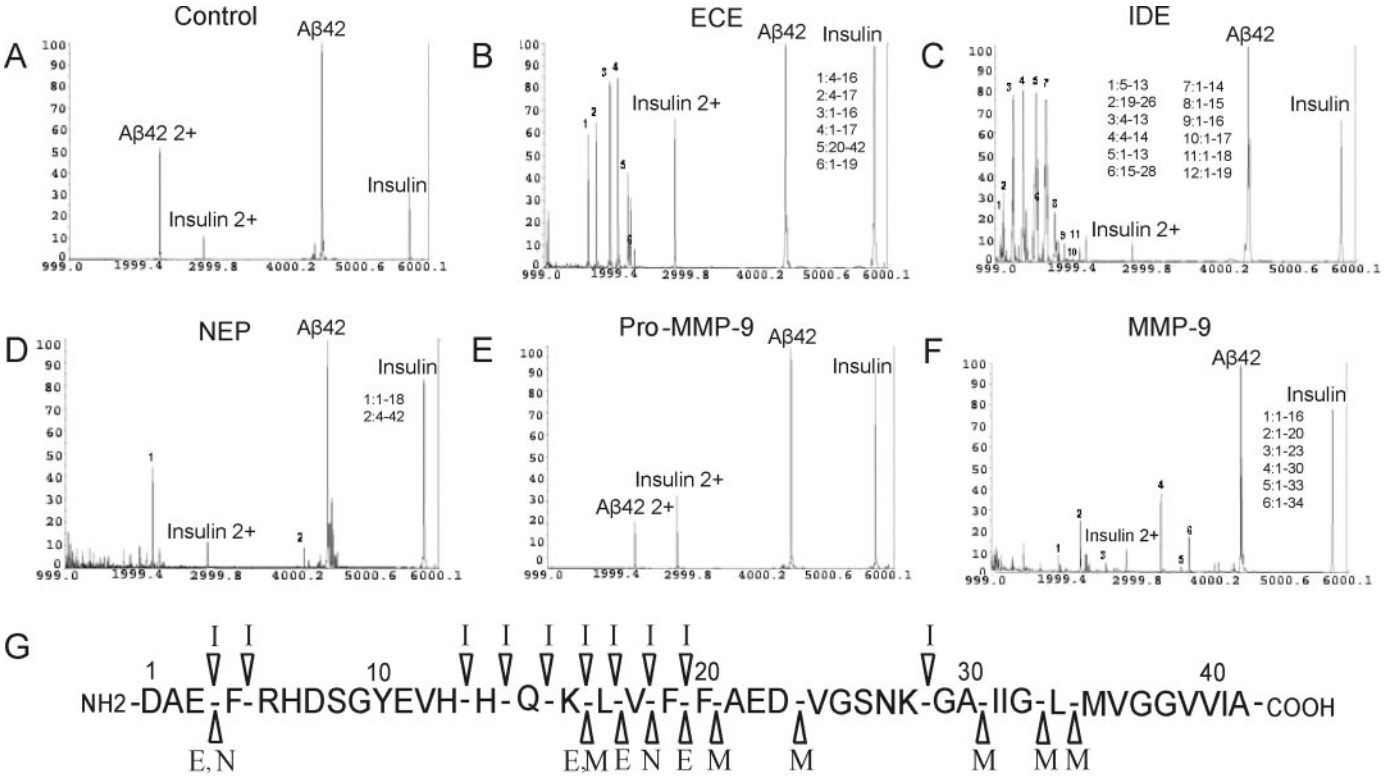

FIGURE 1. Mass spectra of soluble Aβ_{1-42} digested with ECE, IDE, NEP, and MMP-9 (*A–F*). Proteases (100 nM) were incubated with freshly prepared Aβ_{1-42} (2.5 μM) at 37 °C for 4 h, then analyzed using MALDI-TOF MS. Shown are mass spectra of identified fragments of Aβ_{1-42} after digestion with ECE, IDE, NEP, and MMP-9. *G*, summary of the cleavage sites of Aβ_{1-42} degraded by ECE (*E*), IDE (*I*), NEP (*N*), and MMP-9 (*M*).

Immunohistochemistry—APPsw mice (>16 months), APP/PS1 (>6 months), and age-matched wild-type mice were deeply anesthetized and perfused transcardially with 4% paraformaldehyde in 0.1 M phosphate buffer (pH 7.4). Brain cryostat sections (16 μm) were processed for immunofluorescence double labeling, a mixture of rabbit anti-MMP-9 (1:800, gift from Dr. Robert Senior (32) and mouse anti-GFAP (1:2000; Sigma) or pan-Aβ antibody (1:1000; Biosource International) were applied to the sections overnight at 4 °C, then Cy3-conjugated donkey anti-rabbit IgG antibody (1:800; Jackson ImmunoResearch) and Alexa Fluoro 488-conjugated donkey anti-mouse IgG antibody (1:400; Molecular Probes) (33). Sections were coverslipped and examined using confocal microscopy (Zeiss LSM).

In Situ Zymography—Fresh frozen sections (10μ m) were incubated with DQ-gelatin (EnzCheck; Molecular Probes) at a concentration of 0.1 mg/ml in 1% low gel temperature agarose (Sigma) in PBS containing 4′,6-diamidino-2-phenylindole (1.0 μg/ml). Sections were incubated for 24 h at room temperature. For further immunostaining, sections were washed and fixed with ice-cold acetone and alcohol (1:1), then subjected to immunofluorescent staining as described above. Specificity of MMP activity was confirmed by the addition of 20 mM EDTA, which inhibits activity (34).

Statistics—Student's *t* test was employed to determine differences between two groups (ThT comparison ± protease). Paired comparisons (*in situ* plaque degradation assay) were analyzed using the paired *t* test. *p* values <0.05 were considered statistically significant.

RESULTS

Cleavage Sites for Aβ-degrading Proteases—Of the candidate proteases capable of degrading sAβ *in vitro*, only ECE, IDE, and NEP have evidence supporting a role *in vivo* (14–16). To directly compare Aβ-degrading activity and specific peptide fragments generated by digestion between these proteases and MMP-9, freshly prepared synthetic human Aβ_{1-42} or Aβ_{1-40} was incubated with each protease for 4 h prior to analysis with MALDI-TOF MS. Incubation of Aβ_{1-42} with each recombinant human protease (ECE, IDE, NEP, and MMP-9) resulted in relatively specific profiles of Aβ fragments (Fig. 1, *A–F*). The putative Aβ_{1-42} cleavage sites for each protease, based on the fragments generated, are shown in Fig. 1*G*. The major fragments generated from proteolytic cleavage of Aβ_{1-40} were similar to those generated from Aβ_{1-42} (supplemental Fig. 1). In general, the Aβ cleavage sites are in good agreement with previous studies (10, 13, 24, 35, 36). However, a few differences were noted, possibly reflecting differences in the sources of the enzymes used (human *versus* rat), in the nature of Aβ substrate, in the digestion conditions (*e.g.* different buffers), or in detection and purification methods. MMP-9 generated six fragments that, in contrast to other proteases, were mostly in the hydrophobic C-terminal region of the Aβ peptide. All proteases examined exhibited a specific activity for sAβ degradation that was remarkably similar (see below).

MMP-9 Degrades fAβ in Vitro—To determine whether sAβ-degrading proteases could degrade fAβ, human recombinant proteases (ECE, IDE, NEP, and MMP-9) or buffer alone were

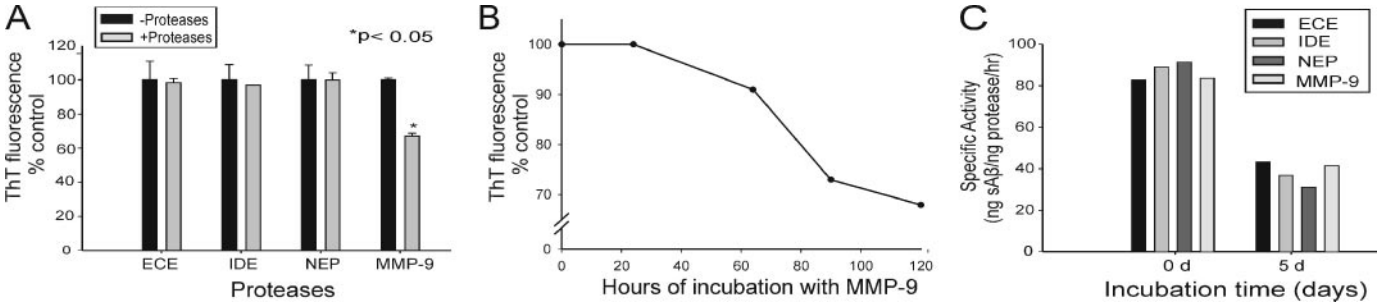

FIGURE 2. **Proteolytic digestion of fAβ_{1-42} with ECE, IDE, NEP, and MMP-9.** *A*, ThT fluorescence was quantified after incubation of fAβ_{1-42} at 37 °C for 5 days with proteases or buffers as indicated. Only MMP-9 digests demonstrated a decrease in ThT fluorescence. *B*, ThT fluorescence decreased in a time-dependent manner after fAβ_{1-42} incubation with MMP-9. *C*, direct comparison of the specific activities of sAβ degradation between different proteases. Proteases, incubated alone (without substrate) at 37 °C for 0 or 5 days, were incubated with freshly prepared Aβ_{1-42} at 37 °C for 4 h and then analyzed by MALDI-TOF MS. Specific activities of ECE, IDE, NEP, and MMP-9 were calculated at 0 and 5 days and were remarkably similar at both time points.

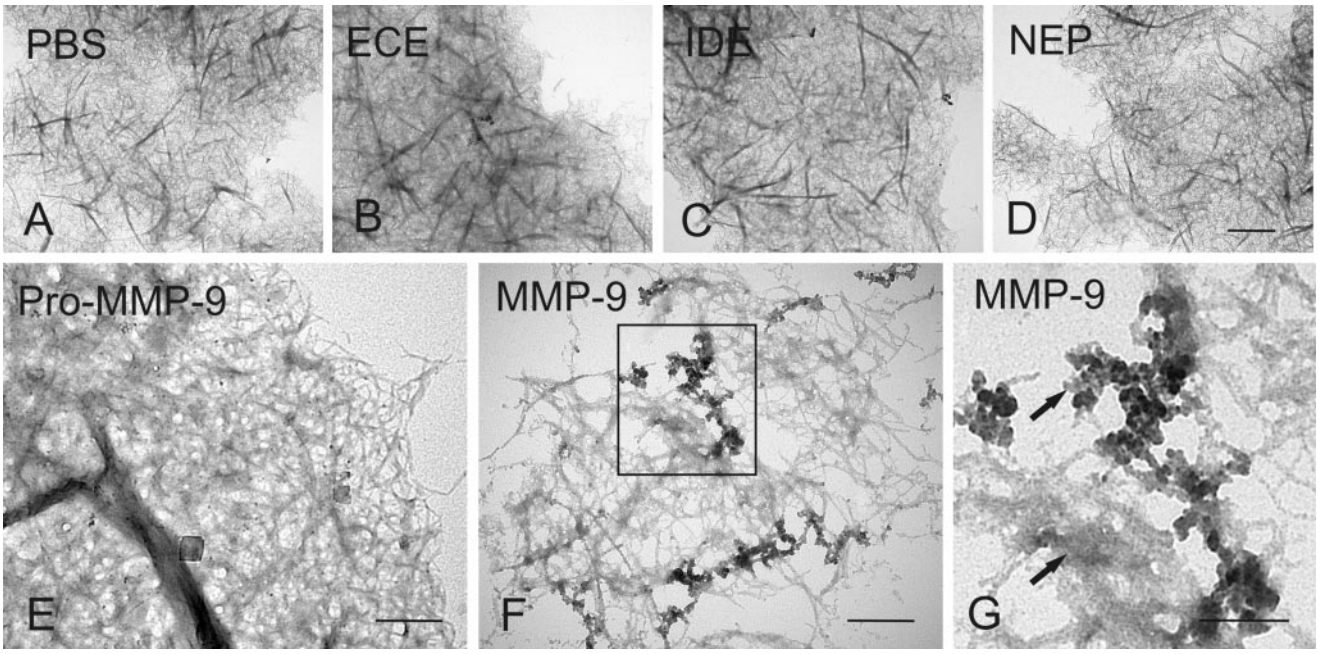

FIGURE 3. **TEM of proteolytically digested fAβ_{1-42}.** After incubating fAβ_{1-42} with PBS or proteases (200 nM) for 5 days at 37 °C, samples were collected for TEM. Amyloid fibrils with approximate diameter of 10 nm were identified; some fibril bundles with diameters of 80–100 nm were also noted. ECE (*B*), IDE (*C*), NEP (*D*), and inactive pro-MMP-9 (*E*) digests did not alter fibril structures as compared with PBS-incubated control samples (*A*). After incubation with activated MMP-9, fibrils were less abundant, and some amorphous globular structures were observed (*F*, *G*), suggestive of decomposed fibrils (*arrows*). *Bars*, 2 μm (*A–D*), 500 nm (*E* and *F*), and 250 nm (*G*).

incubated with preformed Aβ fibrils. These fibrils were formed by incubating Aβ_{1-42} or Aβ_{1-40} at 37 °C for 5 days (see "Experimental Procedures"). For Aβ_{1-42}, ThT fluorescence reached maximal values within 1 day, while Aβ_{1-40} reached maximal fluorescence within 3 days. Preformed Aβ fibrils were then incubated with proteases for 1–5 days at 37 °C and examined using ThT fluorescence. Of the four proteases examined, only MMP-9 reduced ThT fluorescence compared with buffer controls (fAβ_{1-42}, Fig. 2*A*, fAβ_{1-40}; supplemental Fig. 2), suggesting that fAβ was degraded by this protease. This decrease in ThT fluorescence was time-dependent and declined to 70% of initial values by 96 h (Fig. 2*B*). To ensure that similar results could be obtained with Aβ preparations from different batches or manufacturers, we repeated the digestions using fAβ_{1-42} from two different sources (American Peptide and Bachem) and at least two different lots and obtained similar results in each case (data not shown). Because our experiments directly compared the proteolytic activity of four different enzymes, we determined the specific activity for sAβ-degradation using MALDI-TOF MS data after 0 and 5 days of incubating proteases alone (without substrate) at 37 °C. Specific sAβ degrading activity was remarkably similar for all four proteases at 0 days, declining to ~50% after 5 days (Fig. 2*C*). Therefore, the observed differences in fAβ degrading activity did not reflect different specific activities for sAβ degradation among the proteases.

To visualize ultrastructural changes in Aβ fibrils after incubation with proteases, we performed TEM on preformed fAβ incubated in buffer with or without the proteases. TEM of aggregated synthetic human Aβ_{1-42} demonstrated fibrils with an approximate diameter of 10 nm, consistent with prior reports (37, 38). In addition, thicker aggregates of fibers (80–100 nm diameter) were occasionally observed. Incubation of fAβ with ECE, IDE, or NEP, pro-MMP-9 produced no changes compared with PBS alone (Fig. 3, *A–D*), but MMP-9 incubation mixtures contained fewer fibrils. In addition, amorphous structures suggestive of decomposed

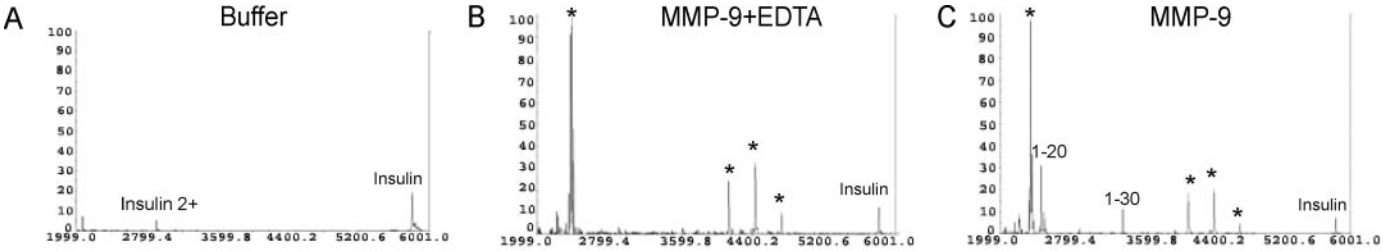

FIGURE 4. **MALDI-TOF MS analysis of Aβ fragment released from fAβ_{1-42} digestion with MMP-9.** Purified fAβ_{1-42} was washed clear of monomer Aβ and fragments using an ultrafiltration unit as described under "Experimental Procedures." After incubation with digestion buffer (*A*) or proteases (300 nM) for 24 h at 37 °C, ultrafiltrate from the digestions were analyzed using MALDI-TOF MS. Aβ fragments were not detected after incubation with ECE, IDE, or NEP (data not shown); however, two fragments were detected after MMP-9 digestion and identified as Aβ fragments 1–20 and 1–30 (*C*). These fragments were not detected in MMP-9 digests inhibited by EDTA (*B*). Four other peaks (labeled *) were identified as contaminants of the MMP-9 preparation and were present in MMP-9-treated samples with (*B*) or without EDTA (*C*), as well as in MMP-9 samples alone (data not shown).

fibrils were observed in the MMP-9 incubation mixtures (Fig. 3, *F* and *G*). These amorphous structures were very similar to that observed for α-helical structures (39) or after Aβ fibril deaggregation with curcumin (30).

To explore the potential mechanisms of fibril disruption by MMP-9, we determined whether Aβ fragments were released by MMP-9 digestion of fAβ. Aβ fragments generated by incubating purified fAβ with ECE, IDE, NEP, or MMP-9 were isolated and analyzed by MALDI-TOF MS. MMP-9 was the only protease examined that produced Aβ fragments (Fig. 4*C*), with molecular masses of 2461.68 and 3390.59 daltons corresponding to Aβ_{1-20} and Aβ_{1-30}. Inhibition of MMP-9 activity with EDTA prevented the generation of Aβ fragments (Fig. 4*B*), suggesting that proteolytic cleavage at Phe^{20}-Ala^{21} or Ala^{30}-Ile^{31} may be important for fibril degradation. Impurities in the MMP-9 preparation are indicated by * and are also seen in the MS of the protease alone (supplemental Fig. 3). Masses of the impurities did not coincide with Aβ fragments.

MMP-9 Degrades Compact Plaques in Situ—Although amyloid plaques are primarily composed of the Aβ peptide, numerous other components are known to colocalize in senile plaques, including proteoglycans, serum constituents, metal ions, and others. Furthermore, posttranslational modifications of Aβ may further stabilize amyloid deposits in plaques (40) Thus, the ability of an enzyme to degrade Aβ fibrils need not imply an ability to degrade amyloid plaques. To determine whether MMP-9 degrades amyloid plaques, we developed a sensitive method to compare the load of compact plaques in adjacent brain sections from aged APP/PS1 mice. Adjacent brain sections were incubated with proteases or buffer alone and then stained with ThS, and the area of fluorescence was compared between matching high power fields from adjacent sections. The area of ThS fluorescence (thioflavin load) in brain sections incubated with ECE, IDE, or NEP did not differ from those incubated with buffer alone, but incubation with MMP-9 resulted in a significant decrease in thioflavin load (Fig. 5*A*–*D*), suggesting that MMP-9 could degrade compact amyloid plaques. Fig. 5*E* illustrates a representative comparison between two corresponding high power fields from adjacent sections (*upper panels*) and the same fields with contrast thresholding to illustrate plaque load (*lower panels*). Note the relative decrease in plaque sizes in the section incubated with MMP-9 (*arrows*, +MMP-9) compared with that incubated with buffer alone (−MMP-9).

MMP-9 Expression and Activity in Brains of APPsw Mice—Unlike other MMPs, MMP-9 is expressed in specific cells at low basal levels, and its expression can be induced by a variety of stimuli, including growth factors, cytokines, reactive oxygen species, or stressors (41). We examined MMP-9 expression in the brains of aged APPsw, APP/PS1, and wild-type littermate mice. Aged wild-type mice demonstrated a few isolated cells with MMP-9 immunoreactivity localized primarily in the corpus callosum (Fig. 6*A*), while APPsw mice had many more cells with prominent MMP-9 immunostaining throughout the brain (including cortex, corpus callosum, and hippocampus, Fig. 6, *B* and *C*). Double staining with ThS revealed that many of the MMP-9 immunoreactive cells appeared to surround ThS-positive compact plaques (Fig. 6*C*). Moreover, the cells had the appearance of activated astrocytes, based on their hypertrophic cell bodies and immunoreactivity with anti-GFAP antibodies (as illustrated by the double labeling experiment in Fig. 6, *D*–*F*). Similar expression profiles were found in 9-month-old APP/PS1 mice (data not shown).

MMP-9 protein expression does not necessarily imply proteolytic activity. MMP-9 activity, like that of other MMPs, is stringently controlled through multiple mechanisms including transcriptional regulation, release from cells, activation through propeptide cleavage, and interaction with TIMPs. Thus, to examine net MMP-9 (gelatinase) activity in the brains of APPsw mice, *in situ* zymography was performed by incubating brain sections with fluorescently labeled gelatin. Gelatinase activity was detected within many but not all amyloid plaques (Fig. 6, *G*–*I*) in aged APPsw mice. Double labeling with ThS and anti-MMP-9 antibodies revealed that the vast majority of plaques with gelatinase activity were ThS-positive compact plaques surrounded by astrocytes expressing MMP-9 (data not shown). Gelatinase fluorescence was inhibited by EDTA even in areas of amyloid plaques (data not shown), suggesting that *in situ* zymography specifically reflects MMP activity.

DISCUSSION

This study provides evidence that MMP-9 is capable of degrading fibrillar Aβ_{1-42}, and this property is not shared by other sAβ-degrading proteases examined (including ECE, ICE, and NEP). MMP-9 incubated with fAβ decreased ThT fluorescence compared with buffer controls. TEM examination of fibrils after digestion with MMP-9 revealed amorphous structures suggestive of disrupted fibrils. Furthermore, MALDI-

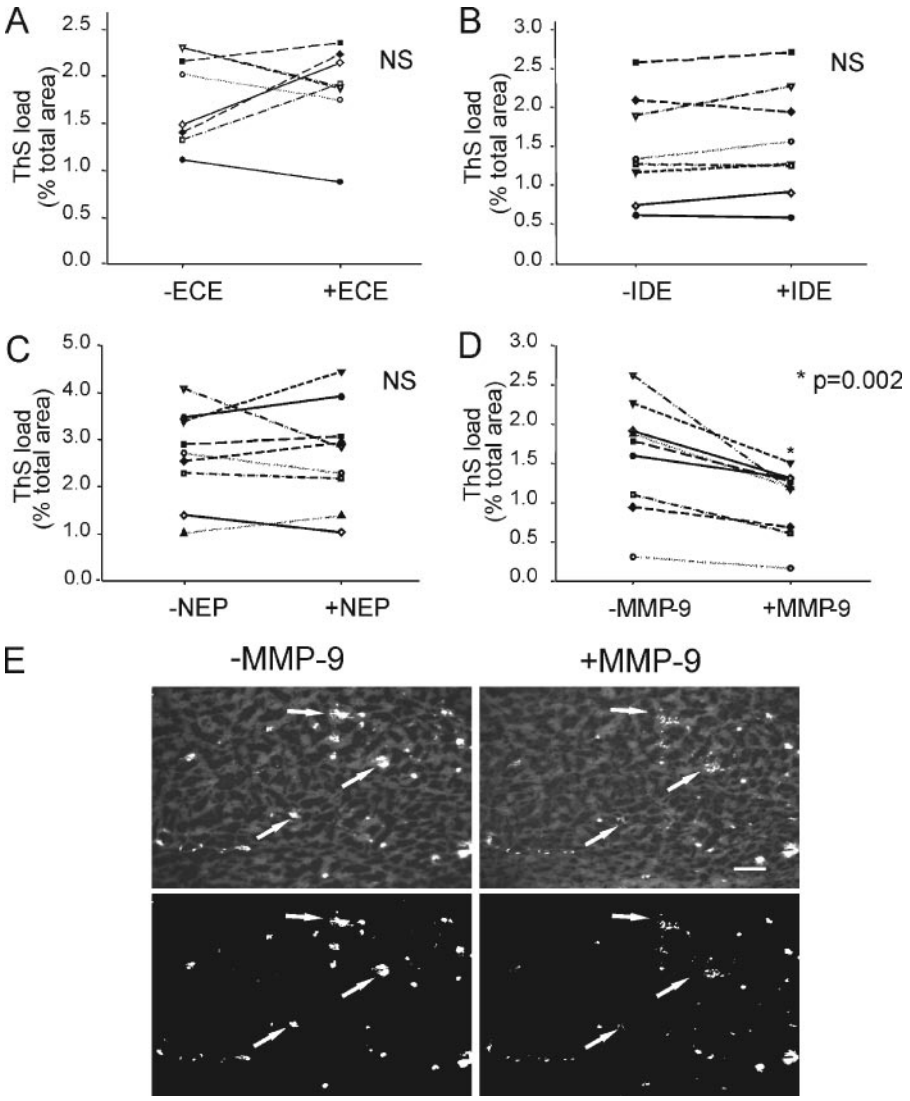

FIGURE 5. ***In situ* compact plaque degradation.** Adjacent 5-μm fresh frozen brain slices from aged APP/PS1 mice were incubated with the indicated proteases (70 nM) or buffer, respectively, at 37 °C for 5 days. Sections were then fixed and stained with ThS, and plaque load was quantified and expressed as percent area per high power field (see "Experimental Procedures"). Incubation with MMP-9 (*D*), but not ECE (*A*), IDE (*B*), or NEP (*C*), decreased the area of ThS staining compared with buffer controls (*, $p < 0.05$, paired *t* test). *E*, a representative example of ThS-stained compact plaques (*arrows*) in adjacent sections incubated with buffer alone (−MMP-9) or with activated MMP-9 (+MMP-9) is shown (*upper panel*). Plaque load was determined using image analysis software after a fixed adjustment of contrast threshold (Sigma Scan, *lower panel*). *Bar*, 100 μm.

TOF MS analyses of MMP-9 digestions demonstrated the appearance of two Aβ fragments (1–20 and 1–30) and established an association between Aβ digestion (at two cleavage sites characteristic of MMP-9) and the breakdown of fibrils. The process of fAβ digestion appeared to be inefficient because ThT fluorescence declined slowly over days. We also demonstrate that MMP-9 is capable of degrading compact amyloid plaques in brain sections from aged APP/PS1 mice. Sensitive analyses of plaque load revealed smaller plaques in brain sections from aged APP/PS1 mice incubated with MMP-9 compared with adjacent section incubated with buffer alone. All of these activities were absent in parallel experiments using ECE, ICE, and NEP, despite the fact that all of the proteases had very similar specific activities for degradation of sAβ.

The fragments of Aβ that were released as fAβ was degraded may provide some insight into the mechanism of fibril cleavage. The precise structure of amyloid fibrils is not yet known, but several structural models have been proposed (42). Common to all of these models is a β-pleated sheet structure perpendicular to the fibril axis (43, 44) with a hairpin loop at the C terminus of Aβ (45). Studies examining different fragments of Aβ demonstrate the importance of two critical regions for aggregation at approximately positions 17–21 and 30–35 (46–48). In our sAβ degradation experiments, MMP-9 demonstrated cleavage sites mainly in the C-terminal hydrophobic region, which contrasted with the other proteases (see Fig. 1). Moreover, fAβ degradation liberated Aβ fragments 1–20 and 1–30, and both cleavage sites are within sequences required for hairpin loop formation and β-sheet structure. Our results also suggest that the cleavage sites Phe^{20}-Ala^{21} and Ala^{30}-Ile^{31} are exposed on the surface of the fibrils in a manner that permits access (albeit inefficient) to MMP-9 for cleavage.

Fibrillar Aβ in compact plaques is believed to be extremely resistant to degradation and clearance, but growing evidence suggests that endogenous mechanisms for plaque clearance exist. The observation that the amyloid plaque size in brains of AD patients does not invariably increase with disease duration suggests an equilibrium between plaque formation and clearance (4, 49). Furthermore, direct observations of amyloid plaques *in vivo* in aged APPsw mice demonstrate that some isolated plaques decrease in size over time (50), suggesting that there are endogenous mechanisms for plaque clearance. Consistent with this view, adult astrocytes incubated on amyloid-laden brain slices from aged PDAPP mice decreased the load of amyloid compared with control slices (51) via an ApoE-dependent mechanism (52). Astrocytes were found to be intimately associated with amyloid plaques in the *in situ* preparations (51) and in post-mortem brain tissue from AD cases (53). In the present study, we have shown that MMP-9 expression is increased in activated astrocytes surrounding diffuse and compact plaques and that gelatinase activity (which reflects MMP activity) resides almost exclusively in compact plaques. Furthermore, we have shown that MMP-9 can degrade compact plaques in an *in situ* degradation assay. These findings suggest that MMP-9 may contribute to astrocyte-mediated amyloid plaque degradation.

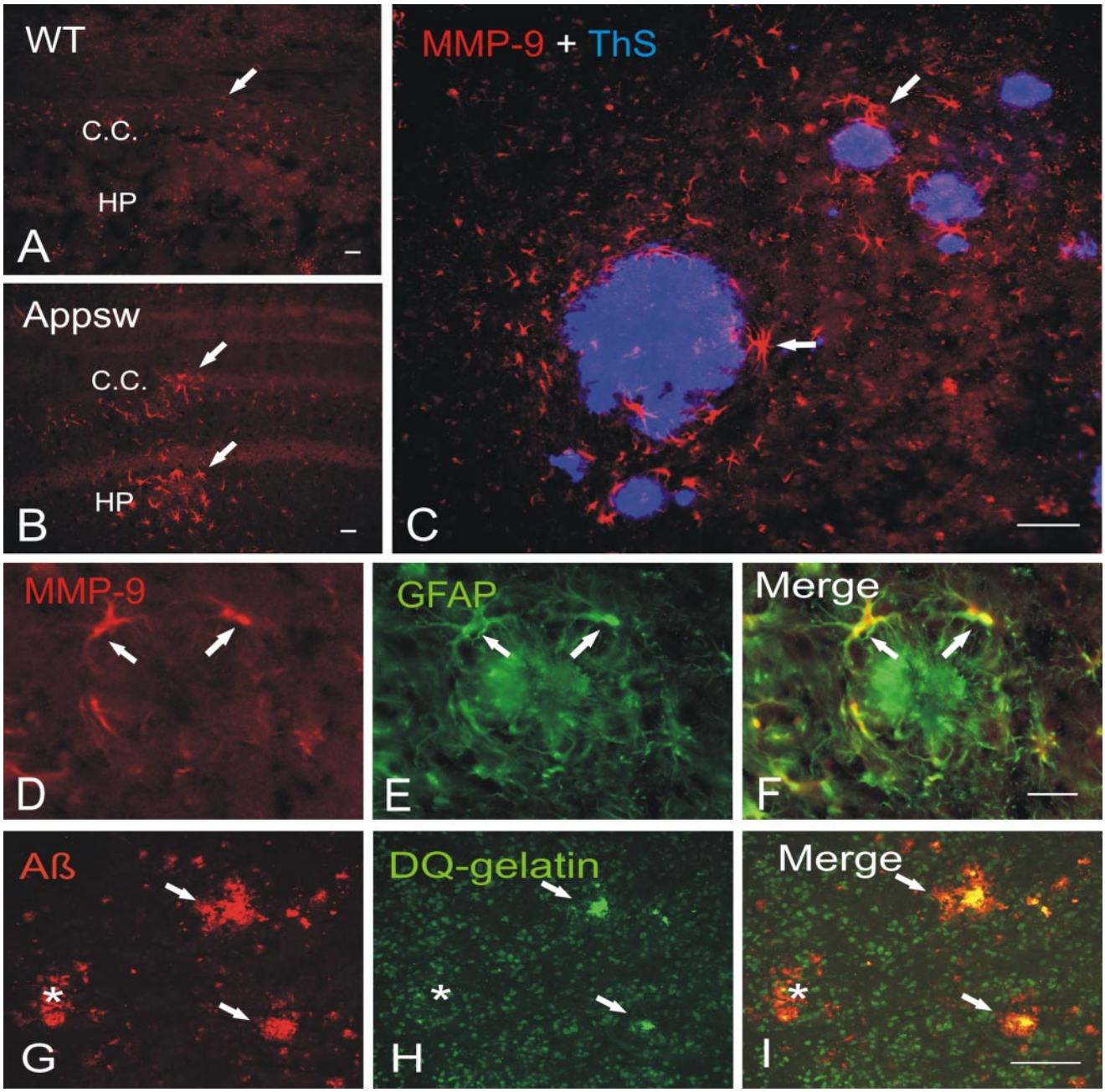

FIGURE 6. **MMP-9-immunoreactivity (*A–F*) and gelatinase activity (*G–I*) in brain sections from 16-month-old wild-type (*WT*, *A*) or APPsw (*B–I*) mice.** Scant MMP-9 immunoreactivity was observed in the corpus callosum (*C.C.*) of aged WT (*A*) mice; however, in APPsw mice (*B*), MMP-9-immunoreactive cells were also observed prominently around Aβ deposits throughout the cortex and hippocampus. Most of these MMP-9-positive cells surrounded ThS-positive plaques (*C*). MMP-9 immunoreactive cells had morphological characteristics of reactive astrocytes (hypertrophic cell bodies with multiple processes) and double labeled with anti-GFAP antibodies (*D–F*). Green fluorescence (*H*), indicative of gelatinase activity, was detected in a subset of Aβ-immunostained plaques (*G–I*; *asterisk* labels a plaque that does not have gelatinase activity, while *arrows* point to two other plaques in the same field showing intense activity). *Bars*, 100 μm (*A* and *B*), 20 μm (*C*), *and 10* μm (*D–I*).

That MMP-9 is expressed in astrocytes surrounding amyloid plaques is consistent with previous reports of MMP-9 expression in neurofibrillary tangles, senile plaques, and in the vascular walls of postmortem brains from AD patients (13, 24), and from APPsw mice (54). Furthermore, *in vitro* studies demonstrate that Aβ induces MMP-9 expression and activity in astrocytes (25, 53). The precise role of activated astrocytes in the pathogenesis of AD is unclear. Some have suggested that astrocytes play a role in plaque formation and exacerbation of injury (53), but others suggest that astroctyes are involved in amyloid clearance (51). Activated astrocytes surrounding amyloid plaques have been shown to secrete a variety of pro-inflammatory molecules, such as interleukins, prostaglandins, leukotrienes, thromboxanes, and proteases (55). MMP-9 expression is frequently increased in pathological inflammatory responses, such as asthma (56), arthritis (57), and multiple sclerosis (58). The precise role of astrocytosis in promoting neurodegeneration *versus* amyloid clearance remains to be delineated.

If proteases such as MMP-9 play a role in degrading fAβ and are expressed in activated astrocytes surrounding plaques, why

do plaques continue to form in disease? One possible explanation is that fAβ-degrading proteases may be overwhelmed by the levels of fAβ in the diseased brain. Based on the time course of fAβ degradation *in vitro*, it appears that this activity of MMP-9 is slow and inefficient, and it might thus be readily overwhelmed. A second possibility is that proteases such as MMP-9 are induced after plaque formation and play a role in limiting plaque growth, causing plaques to reach an equilibrium at a given size. Another explanation may involve aberrant regulation of MMP-9 activity in disease. Like other MMPs, the net activity of MMP-9 depends on several factors, including expression level, release from cells, proteolytic activation, and interaction with endogenous inhibitors (TIMPs). Any of these regulatory processes could be altered in AD. One example is the expression of TIMP-1, the specific inhibitor of MMP-9, which has been reported to be increased in the CSF of AD patients (59).

In this study, we also demonstrate that MMP-9 is capable of degrading sAβ with several cleavage sites toward the C terminus of the peptide. Therefore, like ECE, IDE, and NEP, MMP-9 may also play a role in the degradation and clearance of sAβ *in vivo*. Indeed, we have evidence that steady-state levels of Aβ are lower in the brains of MMP-9 knock-out mice compared with wildtype controls.[4]

In summary, we demonstrate that MMP-9 can degrade fAβ and compact plaques and that this ability is not shared by other proteases examined here. Furthermore, MMP-9 is expressed in astrocytes surrounding plaques in the brains of aged APP/PS1 mice, and its activity is specifically detected in compact plaques. It is likely that other proteases may possess similar activity. Our findings contribute to accumulating evidence that endogenous mechanisms for clearing compact plaque exist. A better understanding of these mechanisms may identify potential therapeutic targets for this incurable disease.

Acknowledgments—We are grateful to Dr. Robert Senior for providing the MMP-9 antibody and Dr. Karen Hsiao Ashe for Tg2576 mice.

REFERENCES

1. Lorenzo, A., and Yankner, B. A. (1996) *Ann. N. Y. Acad. Sci.* **777,** 89–95
2. McLaurin, J., Yang, D., Yip, C. M., and Fraser, P. E. (2000) *J. Struct. Biol.* **130,** 259–270
3. Serpell, L. C. (2000) *Biochim. Biophys. Acta* **1502,** 16–30
4. Hyman, B. T., Marzloff, K., and Arriagada, P. V. (1993) *J. Neuropathol. Exp. Neurol.* **52,** 594–600
5. Christie, R. H., Bacskai, B. J., Zipfel, W. R., Williams, R. M., Kajdasz, S. T., Webb, W. W., and Hyman, B. T. (2001) *J. Neurosci.* **21,** 858–864
6. Cruz, L., Urbanc, B., Buldyrev, S. V., Christie, R., Gomez-Isla, T., Havlin, S., McNamara, M., Stanley, H. E., and Hyman, B. T. (1997) *Proc. Natl. Acad. Sci. U. S. A.* **94,** 7612–7616
7. Thal, D. R., Arendt, T., Waldmann, G., Holzer, M., Zedlick, D., Rub, U., and Schober, R. (1998) *Neurobiol. Aging* **19,** 517–525
8. Howell, S., Nalbantoglu, J., and Crine, P. (1995) *Peptides* **16,** 647–652
9. Kurochkin, I. V., and Goto, S. (1994) *FEBS Lett.* **345,** 33–37
10. Eckman, E. A., Reed, D. K., and Eckman, C. B. (2001) *J. Biol. Chem.* **276,** 24540–24548
11. Hu, J., Igarashi, A., Kamata, M., and Nakagawa, H. (2001) *J. Biol. Chem.* **276,** 47863–47868
12. Tucker, H. M., Kihiko, M., Caldwell, J. N., Wright, S., Kawarabayashi, T., Price, D., Walker, D., Scheff, S., McGillis, J. P., Rydel, R. E., and Estus, S. (2000) *J. Neurosci.* **20,** 3937–3946
13. Backstrom, J. R., Lim, G. P., Cullen, M. J., and Tokes, Z. A. (1996) *J. Neurosci.* **16,** 7910–7919
14. Iwata, N., Tsubuki, S., Takaki, Y., Shirotani, K., Lu, B., Gerard, N. P., Gerard, C., Hama, E., Lee, H. J., and Saido, T. C. (2001) *Science* **292,** 1550–1552
15. Eckman, E. A., Watson, M., Marlow, L., Sambamurti, K., and Eckman, C. B. (2003) *J. Biol. Chem.* **278,** 2081–2084
16. Farris, W., Mansourian, S., Chang, Y., Lindsley, L., Eckman, E. A., Frosch, M. P., Eckman, C. B., Tanzi, R. E., Selkoe, D. J., and Guenette, S. (2003) *Proc. Natl. Acad. Sci. U. S. A.* **100,** 4162–4167
17. Nagase, H., and Woessner, J. F., Jr. (1999) *J. Biol. Chem.* **274,** 21491–21494
18. Gu, Z., Cui, J., Brown, S., Fridman, R., Mobashery, S., Strongin, A. Y., and Lipton, S. A. (2005) *J. Neurosci.* **25,** 6401–6408
19. Rosenberg, G. A., Cunningham, L. A., Wallace, J., Alexander, S., Estrada, E. Y., Grossetete, M., Razhagi, A., Miller, K., and Gearing, A. (2001) *Brain Res.* **893,** 104–112
20. Zhang, X., Cheng, M., and Chintala, S. K. (2004) *Neurosci. Lett.* **356,** 140–144
21. Anthony, D. C., Ferguson, B., Matyzak, M. K., Miller, K. M., Esiri, M. M., and Perry, V. H. (1997) *Neuropathol. Appl. Neurobiol.* **23,** 406–415
22. Maier, C. M., Hsieh, L., Yu, F., Bracci, P., and Chan, P. H. (2004) *Stroke* **35,** 1169–1174
23. Berman, N. E., Marcario, J. K., Yong, C., Raghavan, R., Raymond, L. A., Joag, S. V., Narayan, O., and Cheney, P. D. (1999) *Neurobiol. Dis.* **6,** 486–498
24. Asahina, M., Yoshiyama, Y., and Hattori, T. (2001) *Clin. Neuropathol.* **20,** 60–63
25. Deb, S., Wenjun Zhang, J., and Gottschall, P. E. (2003) *Brain Res.* **970,** 205–213
26. Hsiao, K., Chapman, P., Nilsen, S., Eckman, C., Harigaya, Y., Younkin, S., Yang, F., and Cole, G. (1996) *Science* **274,** 99–102
27. Stine, W. B., Jr., Dahlgren, K. N., Krafft, G. A., and LaDu, M. J. (2003) *J. Biol. Chem.* **278,** 11612–11622
28. LeVine, H., III (1997) *Arch. Biochem. Biophys.* **342,** 306–316
29. Wang, R., Sweeney, D., Gandy, S. E., and Sisodia, S. S. (1996) *J. Biol. Chem.* **271,** 31894–31902
30. Yang, F., Lim, G. P., Begum, A. N., Ubeda, O. J., Simmons, M. R., Ambegaokar, S. S., Chen, P. P., Kayed, R., Glabe, C. G., Frautschy, S. A., and Cole, G. M. (2005) *J. Biol. Chem.* **280,** 5892–5901
31. Sun, A., Nguyen, X. V., and Bing, G. (2002) *J. Histochem. Cytochem.* **50,** 463–472
32. Betsuyaku, T., Fukuda, Y., Parks, W. C., Shipley, J. M., and Senior, R. M. (2000) *Am. J. Pathol.* **157,** 525–535
33. Yan, P., Xu, J., Li, Q., Chen, S., Kim, G. M., Hsu, C. Y., and Xu, X. M. (1999) *J. Neurosci.* **19,** 9355–9363
34. Goussev, S., Hsu, J. Y., Lin, Y., Tjoa, T., Maida, N., Werb, Z., and Noble-Haeusslein, L. J. (2003) *J. Neurosurg.* **99,** 188–197
35. Morelli, L., Llovera, R., Gonzalez, S. A., Affranchino, J. L., Prelli, F., Frangione, B., Ghiso, J., and Castano, E. M. (2003) *J. Biol. Chem.* **278,** 23221–23226
36. Iwata, N., Tsubuki, S., Takaki, Y., Watanabe, K., Sekiguchi, M., Hosoki, E., Kawashima-Morishima, M., Lee, H. J., Hama, E., Sekine-Aizawa, Y., and Saido, T. C. (2000) *Nat. Med.* **6,** 143–150
37. Shirahama, T., and Cohen, A. S. (1967) *J. Cell Biol.* **33,** 679–708
38. Serpell, L. C., Blake, C. C., and Fraser, P. E. (2000) *Biochemistry* **39,** 13269–13275
39. Nilsson, M. R. (2004) *Methods* (*Amst.*) **34,** 151–160
40. Atwood, C. S., Martins, R. N., Smith, M. A., and Perry, G. (2002) *Peptides* **23,** 1343–1350
41. Van den Steen, P. E., Dubois, B., Nelissen, I., Rudd, P. M., Dwek, R. A., and Opdenakker, G. (2002) *Crit. Rev. Biochem. Mol. Biol.* **37,** 375–536
42. Wetzel, R. (2002) *Structure* (*Camb.*)**10,** 1031–1036

[4] K. Yin, J. R. Cirrito, P. Yan, X. Hu, Q. Xiao, X. Pan, R. Bateman, H. Song, F. Hsu, J. Turk, J. Xu, C. Y. Hsu, J. C. Mills, D. M. Holtzman, and J. M. Lee, submitted for publication.

43. Inouye, H., Fraser, P. E., and Kirschner, D. A. (1993) *Biophys. J.* **64,** 502–519
44. Sunde, M., Serpell, L. C., Bartlam, M., Fraser, P. E., Pepys, M. B., and Blake, C. C. (1997) *J. Mol. Biol.* **273,** 729–739
45. Shivaprasad, S., and Wetzel, R. (2004) *Biochemistry* **43,** 15310–15317
46. Hilbich, C., Kisters-Woike, B., Reed, J., Masters, C. L., and Beyreuther, K. (1992) *J. Mol. Biol.* **228,** 460–473
47. Liu, R., McAllister, C., Lyubchenko, Y., and Sierks, M. R. (2004) *J. Neurosci. Res.* **75,** 162–171
48. Bond, J. P., Deverin, S. P., Inouye, H., el-Agnaf, O. M., Teeter, M. M., and Kirschner, D. A. (2003) *J. Struct. Biol.* **141,** 156–170
49. Arriagada, P. V., Growdon, J. H., Hedley-Whyte, E. T., and Hyman, B. T. (1992) *Neurology* **42,** 631–639
50. Bacskai, B. J., Kajdasz, S. T., Christie, R. H., Carter, C., Games, D., Seubert, P., Schenk, D., and Hyman, B. T. (2001) *Nat. Med.* **7,** 369–372
51. Wyss-Coray, T., Loike, J. D., Brionne, T. C., Lu, E., Anankov, R., Yan, F., Silverstein, S. C., and Husemann, J. (2003) *Nat. Med.* **9,** 453–457
52. Koistinaho, M., Lin, S., Wu, X., Esterman, M., Koger, D., Hanson, J., Higgs, R., Liu, F., Malkani, S., Bales, K. R., and Paul, S. M. (2004) *Nat. Med.* **10,** 719–726
53. Nagele, R. G., Wegiel, J., Venkataraman, V., Imaki, H., and Wang, K. C. (2004) *Neurobiol. Aging* **25,** 663–674
54. Lee, J. M., Yin, K. J., Hsin, I., Chen, S., Fryer, J. D., Holtzman, D. M., Hsu, C. Y., and Xu, J. (2003) *Ann. Neurol.* **54,** 379–382
55. McGeer, E. G., and McGeer, P. L. (2001) *Mol. Interv.* **1,** 22–29
56. Kelly, E. A., and Jarjour, N. N. (2003) *Curr. Opin. Pulm. Med.* **9,** 28–33
57. Iannone, F., and Lapadula, G. (2003) *J. Rheumatol.* **30,** 2294–2295
58. Dubois, B., Opdenakker, G., and Carton, H. (1999) *Acta Neurol. Belg.* **99,** 53–56
59. Lorenzl, S., Albers, D. S., LeWitt, P. A., Chirichigno, J. W., Hilgenberg, S. L., Cudkowicz, M. E., and Beal, M. F. (2003) *J. Neurol. Sci.* **207,** 71–76